RESEARCH

Changes in epigenetic profiles throughout early childhood and their relationship to the response to pneumococcal vaccination

Sara Pischedda[1,2,3*†] , Daniel O'Connor[4*†] , Benjamin P. Fairfax[5] , Antonio Salas[1,3] , Federico Martinon-Torres[1,2] , Andrew J. Pollard[4] and Johannes Trück[4,6*]

Abstract

Background: Pneumococcal infections are a major cause of morbidity and mortality in young children and immaturity of the immune system partly underlies poor vaccine responses seen in the young. Emerging evidence suggests a key role for epigenetics in the maturation and regulation of the immune system in health and disease. The study aimed to investigate epigenetic changes in early life and to understand the relationship between the epigenome and antigen-specific antibody responses to pneumococcal vaccination.

Methods: The epigenetic profiles from 24 healthy children were analyzed at 12 months prior to a booster dose of the 13-valent pneumococcal conjugate vaccine (PCV-13), and at 24 months of age, using the Illumina Methylation 450 K assay and assessed for differences over time and between high and low vaccine responders.

Results: Our analysis revealed 721 significantly differentially methylated positions between 12 and 24 months (FDR < 0.01), with significant enrichment in pathways involved in the regulation of cell–cell adhesion and T cell activation. Comparing high and low vaccine responders, we identified differentially methylated CpG sites (*P* value < 0.01) associated with *HLA-DPB1* and *IL6*.

Conclusion: These data imply that epigenetic changes that occur during early childhood may be associated with antigen-specific antibody responses to pneumococcal vaccines.

Keywords: Pneumococcal vaccination, Immune system, Childhood, Vaccine response, Epigenetics, DNA methylation

*Correspondence: sara.pischedda01@gmail.com; daniel.oconnor@paediatrics.ox.ac.uk; johannes.trueck@kispi.uzh.ch

†Sara Pischedda and Daniel O'Connor have contributed equally to this work

1 Genetics, Vaccines and Infections and Pediatrics Research Group (GENVIP), Instituto de Investigación Sanitaria de Santiago, Santiago de Compostela, Spain

4 Oxford Vaccine Group, Department of Paediatrics, University of Oxford, and The NIHR Oxford Biomedical Research Centre, Oxford, UK

Full list of author information is available at the end of the article

Background

Young children are at higher risk of developing life-threatening diseases compared with adults, which is thought to be due to the immaturity of their immune system. They also show reduced immune responses to vaccines [1]. Pneumococcal infections are a major public health problem worldwide causing high morbidity and mortality in young children who suffer pneumonia, meningitis and septicemia, leading up to 1 million deaths in children under the age of five years [2, 3]. Despite many years of research, the specific

Pischedda *et al. Clin Epigenet*   (2021) 13:29

Page 2 of 12

characteristics of the immune system in early childhood that underpins increased susceptibility to infection has still not been fully elucidated [4]. Furthermore, there is great variability in the immune response to vaccination in children, with some individuals achieving more than 100-fold higher antibody levels post-immunization than others [5, 6]. The reason for this huge variation is not understood, and recent studies have begun to reveal the genetic determinants of immune responses to vaccines [7, 8].

The term epigenetics or 'the epigenome' describes the summary of heritable changes in expression (i.e., function) of genes that are not encoded in the DNA sequence and form a mechanism whereby past environmental events may be encoded and modify future cellular responses. Epigenetic mechanisms have repressive and permissive effects on gene expression and thus play a key role in cellular differentiation. DNA methylation forms the archetypal, heritable, epigenetic mark and involves the chemical modification of cytosine and cytosine:guanine dinucleotides, resulting in profound, typically repressive, effects [9]. DNA methylation patterns can be measured across the whole genome covering 99% of currently annotated genes in a high-throughput manner [10]. They differ between individuals, even between identical twins, and their change over time is influenced by intrauterine and postnatal environmental factors such as nutrition, toxins or drugs and illnesses [11]. Recent studies have demonstrated that the levels of DNA methylation of certain CpG sites are also highly correlated with human chronological age [12]. Moreover, these DNA methylation features have been proposed as a surrogate of the "biological age," which may actually be more relevant than chronological age in predicting age-related health risks [13]. Different conditions have been reported to accelerate age-associated DNA methylation profiles such as HIV infection and Down syndrome [14, 15].

There is increasing evidence demonstrating a key role of epigenetics in regulation of human immunity in health and disease [16, 17]. Consistent with this, DNA methylation changes during early childhood have been observed in genes implicated in inflammatory processes, encoded histone modifiers and chromatin remodeling factors [18]. However, the effects of these changes on the immune system are unknown. Importantly, there is limited information on the relationship between epigenetic changes in infancy and the response to vaccination. Here, we sought to investigate epigenetic changes in early life in a well-studied cohort of healthy children, focusing on the characterization of the relationship between epigenetics and age in paired samples collected at 12 and 24 months of age, and the role of epigenetics on the strength of

antigen-specific antibody responses to pneumococcal vaccination.

Results

Twenty-four children (Table 1) who had received the 13-valent pneumococcal conjugate vaccine (PCV-13) at 12 months of age, as part of a previously published clinical trial [19–21], were selected based on their aggregated IgG antibody response and categorized into high and low responders (Fig. 1 and Additional file 1: Figure 1). Of note, this categorization was also valid for post-booster serotype-specific opsonophagocytic assay (OPA) titers and memory B cells responses (Additional file 1: Figures 2 and 3), therefore truly grouping individuals into high and low vaccine responders. Paired blood samples taken at 12 and 24 months of age were assessed by DNA epigenetic microarray analysis.

Widespread changes in the epigenome occur between 12 and 24 months of life

The first step of our analysis focused on the methylation changes between the two timepoints (12 vs. 24 months). After correcting our linear model for cell-type composition, we found 721 significant DMPs, associated with 421 unique genes. Considerable inflation could be observed in the QQ plot (Additional file 1: Figure 4), reflecting substantial age-related changes to the blood epigenome early in life. Of the significant DMPs, 314 (43.6%) were hypomethylated with the remaining 407 (56.4%) being hypermethylated, in samples collected at 12 months of age (Additional file 7: Table 1). The results without adjusting for cell compositions are shown in Additional file 8: Table 2. There was a clear separation between samples from 12 and 24 months of age using PCA and hierarchical clustering of the 721 DMPs (Fig. 2).

Further analyzing the 721 DMPs, we observed several DMRs where multiple adjacent CpGs probes were found together showing differential methylation between the two different timepoints. For instance, 10 probes were associated with nuclear factor I X (*NFIX*), and 12 CpGs were observed within the same island region, chr6:32118101–32118544, of the proline-rich transmembrane protein 1 (*PRRT1*). Hypomethylated CpGs were mainly found in CpG islands, whereas open sea, shore and shelf regions were mostly hypermethylated (Additional file 5: Figure 5a). Most DMPs were found in the gene body, TSS1500 and 5′ UTRs and dominated by hypomethylation patterns (Additional file 1: Figure 5b).

We further analyzed DMPs, which showed the highest age-dependent differences in methylation by applying a delta beta (difference in the mean β value of each group) threshold of ≥ 0.10. In this way, we detected 24 DMPs, considered as the DMPs most separating the two

Pischedda *et al. Clin Epigenet*   (2021) 13:29

Page 3 of 12

Table 1 Characteristics of study participants

Pneumococcal vaccine response	Sex	Age at visit 1 (months)	Age at visit 3 (months)	Ethnicity
High	f	12.46	23.82	Indian/British
High	f	12.16	23.46	European/White west African
High	f	12.43	23.72	White Caucasian/European
High	f	12.75	24.05	White Caucasian/European
High	f	12.2	23.98	White Caucasian/European
High	m	12.72	24.57	White Caucasian/European
High	m	11.77	23.52	White Caucasian/European
High	m	12.72	24.25	White Caucasian/European
High	m	13.28	24.61	White Caucasian/European
High	m	12.75	24.28	White Caucasian/European
High	m	12.82	24.61	White Caucasian/European
High	m	12.85	24.08	White Caucasian/European
Low	f	12.56	23.89	White Caucasian/European
Low	f	12.49	23.85	White Caucasian/European
Low	m	12.39	23.95	White Caucasian/European
Low	m	12.16	23.66	Asian South East Asian Heritage
Low	m	12.98	24.74	White Caucasian/European
Low	m	12.39	23.46	White Caucasian/European
Low	m	12.00	23.26	White Caucasian/European
Low	m	13.05	24.38	White South African
Low	m	12.46	23.49	White Caucasian/European
Low	m	12.36	24.21	Canadian/British
Low	m	13.18	24.51	White Caucasian/European
Low	m	12.92	24.9	White Caucasian/European

f female, *m* male

age groups (Table 2); of those, 18 CpGs exhibited a higher methylation level at 24 months, while the remaining 6 had a lower methylation pattern at 24 months.

Age-associated changes in the epigenome are enriched for pathways linked to T cell regulation and activation

To investigate which molecular functions or biological processes were associated with the DMPs between 12 and 24 months of age, gene set enrichment analysis was performed. We detected significant enrichment (FDR < 0.05) in 151 GO pathways, with the most significant pathways being related to regulation of T cell activation, cell–cell adhesion and regulation of cytokine production (Fig. 3; Additional file 9: Table 3).

Among DMPs, we observed 86 CpGs associated with 69 unique genes within immune system processes according to GO terms. Of these, 53 CpGs showed a decrease in methylation with age, while the other 32 exhibited an increase in methylation from 12 to 24 months (Fig. 4). Some of the genes were represented by multiple DMPs, such as *HOXB6*, *NOD2* and *LAG3*, in the latter we found both hypo- and hypermethylated CpGs.

In order to understand if the different responsiveness to vaccination was associated with the "biological age" of the subjects, we used the epigenetic age estimator developed by Horvath in 2013 [22] to calculate biological age based on methylation patterns. First, we applied age predictors to the results obtained from samples at the two time points and found that chronological and predicted biological ages were correlated (Fig. 5a). We did not observe significant differences in predicted biological age between high and low vaccine responders (Fig. 5b).

Hypomethylation of HLA-DPB1 and hypermethylation of IL-6 is associated with more robust responses to pneumococcal infant vaccination

We next assessed whether differences in antibody responses against vaccine antigens were associated with methylation patterns by comparing pre-vaccination blood epigenome profiles of high responders to those of low responders. After applying a FDR < 0.01 correction, no statistically significant DMPs were detected. However, using a less stringent statistical threshold (uncorrected *P* value < 0.01), we found 4067 differentially

Pischedda *et al. Clin Epigenet*   *(2021) 13:29*

Page 4 of 12

Fig. 1 Study design including sample selection for epigenetic studies and overview of main results

Fig. 2 **a** Principal component analysis and **b** heatmap including unsupervised clustering of age (24 vs. 12 months) using the 721 significant differentially methylated positions

Pischedda *et al. Clin Epigenet* (2021) 13:29

Page 5 of 12

Table 2 List of the 24 DMPs with an absolute difference in methylation levels > 0.10 between 12 and 24 months of age

CpG_ID	Chr	Position	Relation to CGI	Gene name	Gene group	FDR *P* value	Mean value (m12–m24)
cg05825244	chr20	2,730,488	Island	EBF4	Body	2.96E−04	− 0.2201
cg25556035	chr19	13,127,873	S_Shelf	NFIX	Body	4.27E−07	− 0.1930
cg14716990	chr10	129,533,731	N_Shore			9.20E−08	− 0.1523
cg22268510	chr6	32,118,420	Island	PRRT1	Body	5.14E−07	− 0.1448
cg10767662	chr19	13,127,729	S_Shelf	NFIX	Body	3.43E−07	− 0.1407
cg01323777	chr17	7,832,943	Island	KCNAB3	TSS200	4.09E−05	− 0.1366
cg00254681	chr6	32,118,457	Island	PRRT1	Body	1.01E−06	− 0.1321
cg13138089	chr2	233,251,770	Island	ECEL1P2	TSS200	7.75E−03	− 0.1309
cg13870494	chr9	72,658,358	N_Shore	MAMDC2	TSS200	2.36E−05	− 0.1244
cg20471691	chr17	46,681,316	N_Shelf	LOC404266; LOC404266; HOXB6	Body; body; 5′UTR	4.05E−05	− 0.1164
cg23365801	chr17	7,832,909	Island	KCNAB3	TSS200	8.93E−04	− 0.1163
cg23491743	chr2	241,989,271	Island	SNED1	Body	2.15E−06	− 0.1141
cg27162435	chr17	7,833,163	Island	KCNAB3	TSS1500	8.86E−05	− 0.1099
cg00589520	chr7	23,513,039	N_Shore			1.15E−09	− 0.1053
cg09490371	chr2	233,253,024	Island	ECEL1P2	TSS1500	2.54E−03	− 0.1051
cg11617964	chr6	32,118,399	Island	PRRT1	Body	1.82E−08	− 0.1027
cg25460807	chr8	21,908,022	S_Shelf			6.25E−04	− 0.1013
cg11041817	chr17	46,685,327	Island	HOXB7	Body	4.88E−03	− 0.1011
cg16146033	chr11	62,767,323	OpenSea	SLC22A8	Body	5.40E−08	0.1063
cg02481642	chr20	43,343,760	OpenSea	WISP2	TSS200	5.78E−06	0.1085
cg25135018	chr1	154,435,948	OpenSea	IL6R; IL6R	Body; body	1.16E−06	0.1099
cg06688910	chr8	122,466,955	OpenSea			6.72E−08	0.1101
cg17945323	chr11	62,767,406	OpenSea	SLC22A8	Body	6.66E−09	0.1103
cg09978533	chr22	46,465,160	N_Shore			9.39E−06	0.1149

The top 18 CpGs are hypermethylated, while the bottom 6 CpGs are hypomethylated in samples from 24 months compared with 12 months of age

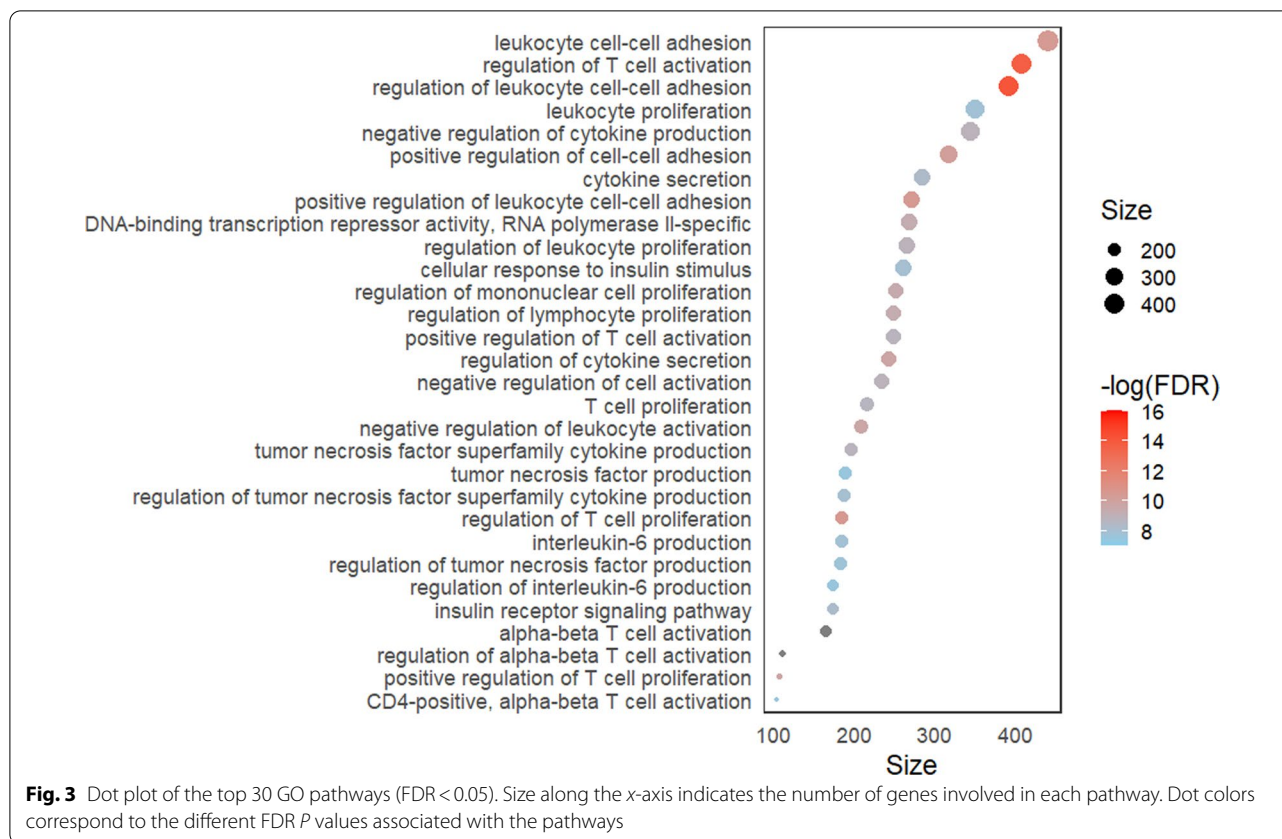*Chr* chromosome, **N_Shore/N_Shel* North Shore/Shelf, *S_Shore/S_Shelf* South Shore/Shelf

methylated CpG sites (Additional file 10: Table 4) associated with 2797 unique genes that distinguished high from low responders in a PCA (Fig. 6a) and an unsupervised clustering method (Fig. 6b). Similar results were obtained for a group comparison at 24 months (Additional file 6: Figure 6).

We further investigated among the 4067 DMPs those which showed the highest difference in methylation between high and low vaccine responders (mean β value) and assessed regions containing multiple DMPs in genes involved in immune system processes. Among the top DMPs identified, there were 4 hypomethylated positions in high vaccine responders within the chr6:33048416−33048814 island region of the HLA class II histocompatibility antigen DP(W2) beta chain (*HLA-DPB1*). There were also two CpGs associated with interleukin 6 (*IL-6*) that showed hypermethylation in high compared with low vaccine responders (Fig. 6c).

Discussion

In the present study, we demonstrated age-associated DNA methylation changes between the first and second year of life that were largely related to T cell regulation and activation. In addition, using detailed antibody measurements following infant pneumococcal conjugate booster vaccination in a clinical vaccine trial, we found hypomethylation of *HLA-DPB1* and hypermethylation of *IL6* to be correlated with a stronger response to pneumococcal vaccination.

A total of 721 CpGs were found to be significantly differentially methylated between 12 and 24 months of age. Multiple DMPs within several DMRs showed similar methylation patterns suggesting a general epigenetic remodeling of these genetic loci. For example, within the chr6:32118101−32118544 locus, there were twelve DMPs that exhibited a significantly higher methylation pattern at 24 compared with 12 months of age. These DMPs are

Pischedda *et al. Clin Epigenet*   (2021) 13:29

Page 6 of 12

Fig. 3 Dot plot of the top 30 GO pathways (FDR < 0.05). Size along the *x*-axis indicates the number of genes involved in each pathway. Dot colors correspond to the different FDR *P* values associated with the pathways
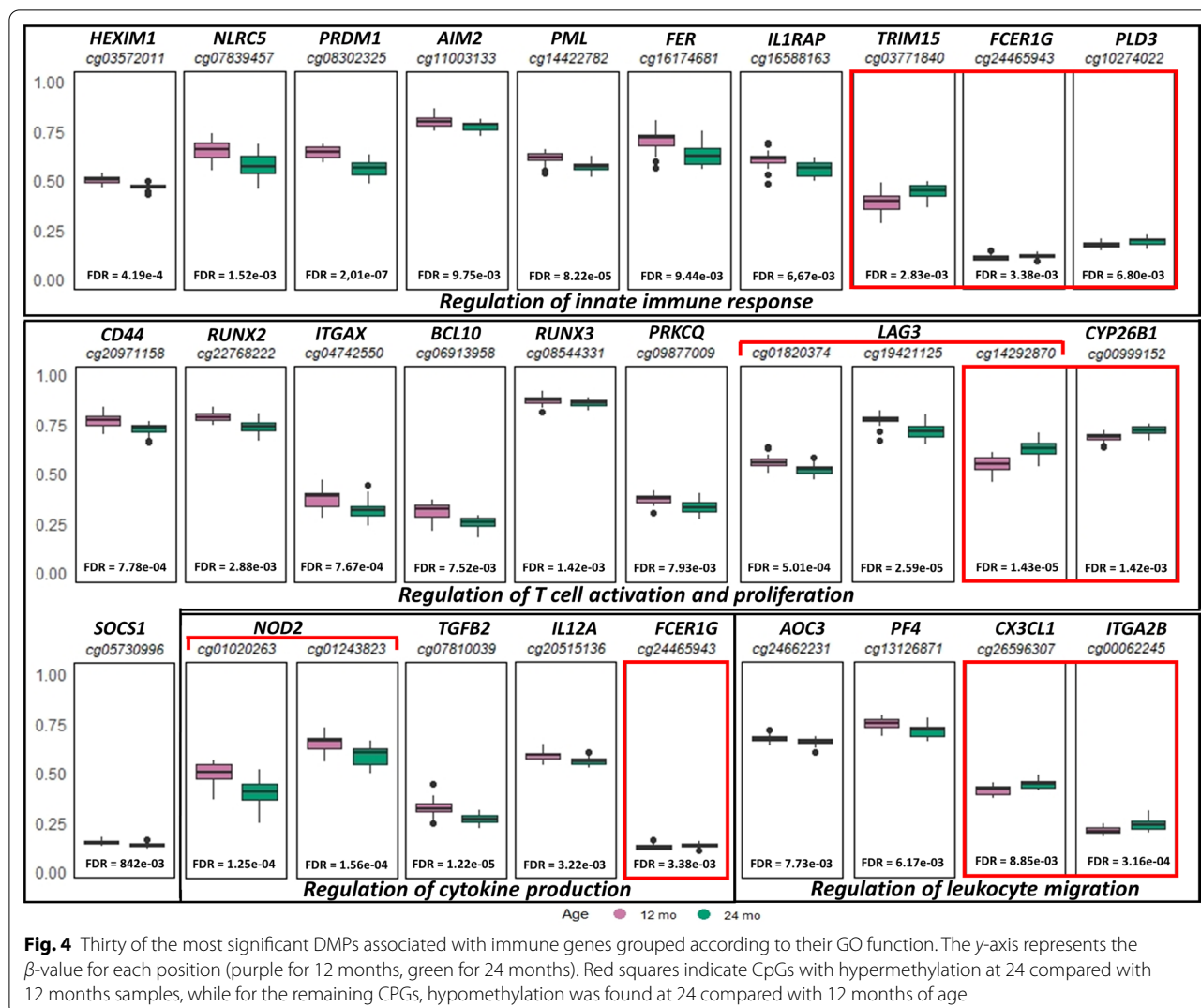
localized within the body of *PRRT1* and could potentially alter the expression of *PRRT1*, as previously demonstrated for other hypermethylated positions in genes outside of the promoter area [23]. Little is known about the function of *PRRT1* although aberrant methylation of this gene has been related to neurodevelopmental disorders [24] and to hepatic tumorigenesis [25]. Furthermore, we observed a total of 118 CpGs that were previously reported to be altered between 3 and 60 months in blood leukocytes [18]. In agreement with this previous work, we observed 57 CpGs exhibiting an increase in methylation between 12 and 24 months of age, and 60 CpGs showing a decreased methylation with age [18].

Through an enrichment pathway analysis of the age dependent DMPs, we observed 86 CpGs that were associated with 69 genes involved in several immune system processes. Genes that were hypomethylated at 24 compared with 12 months included *IL12A*, previously shown to be repressed at chromatin level in neonatal mononuclear compared with adult cells [26–28], as well as *BCL10* and *NOD2*, also previously demonstrated to decrease methylation with age [18]. In contrast, CpGs with an increase in methylation between 12 and 24 months included genes involved in the regulation of innate immune responses such as tripartite motif

containing 15 (*TRIM15*) [30], and the PML Nuclear Body Scaffold (*PML*) [31]. A particular pattern of methylation was observed for lymphocyte activating 3 (*LAG3)*, also required for T cell regulation [32]. *LAG3* was hypomethylated at two positions within the chr12:6882855–6883184 region and hypermethylated in an open sea CpG at 24 months, suggesting that diverging methylation patterns may regulate expression of this gene.

There was a clear separation of predicted biological age between samples taken at the two study time points. Predicted biological age was moderately higher than chronological age, most likely due to the small range of errors for whole blood samples that the age predictor exhibits [22]. However, predicted biological age was not significantly different between high and low vaccine responders at any time point suggesting no differences attributable to "epigenetic age" between the groups.

The second part of our research study focused on the relationship between the epigenome at 12 months of age before immunization and the strength of the antigen-specific IgG response to vaccination. We identified a high number of CpGs that separated high from low vaccine responders using a less stringent statistical threshold (uncorrected *P* value <0.01). These CpGs included multiple probes mapping to genes involved in immune system

Fig. 4 Thirty of the most significant DMPs associated with immune genes grouped according to their GO function. The *y*-axis represents the *β*-value for each position (purple for 12 months, green for 24 months). Red squares indicate CpGs with hypermethylation at 24 compared with 12 months samples, while for the remaining CPGs, hypomethylation was found at 24 compared with 12 months of age

processes and were associated with large differences in methylation between the two groups. In this way, we observed two particularly interesting immune genes (*HLA-DPB1* and *IL6*) that contained multiple DMPs differing between high and low vaccine responders. Hypomethylation of *HLA-DPB1* as found in high compared with low vaccine responders may indeed strengthen the overall immune response as previously demonstrated by the contribution of HLA to cellular host immunity in response to anthrax vaccine adsorbed [33]; rubella vaccine [34]; hepatitis B vaccine; and the inactivated Japanese encephalitis vaccine [35]. Additional evidence connecting HLA genotype and expression to vaccine immune responses was found in measles seropositive and seronegative individuals [36]. Two CpGs in the body of *IL6* showed higher methylation in high compared with low vaccine responders. These CpGs in open sea positions (i.e., isolated in the genome [37]) are considered

to be "predicted enhancer elements" [38], therefore possibly impacting *IL6* expression. Il-6 is a proinflammatory cytokine involved in a variety of immune processes and also plays an important role in mediating innate and adaptive immune responses [39]; therefore, differential expression of *IL6* may impact vaccine immune responses. However, in contrast to our finding of hypermethylated (and possibly reduced expression of) *IL6* in high vaccine responders, previous work suggested that IL-6 promotes stimulation of humoral and cellular immune responses [40–43].

There are several limitations to our study. First, several samples had to be excluded due to unavailability of genetic material, consent for genetic analysis or missing serum, which may have affected the results. In addition, high and low responders were categorized using the aggregated serotype-specific IgG response 1-month post-booster vaccination, which may not accurately
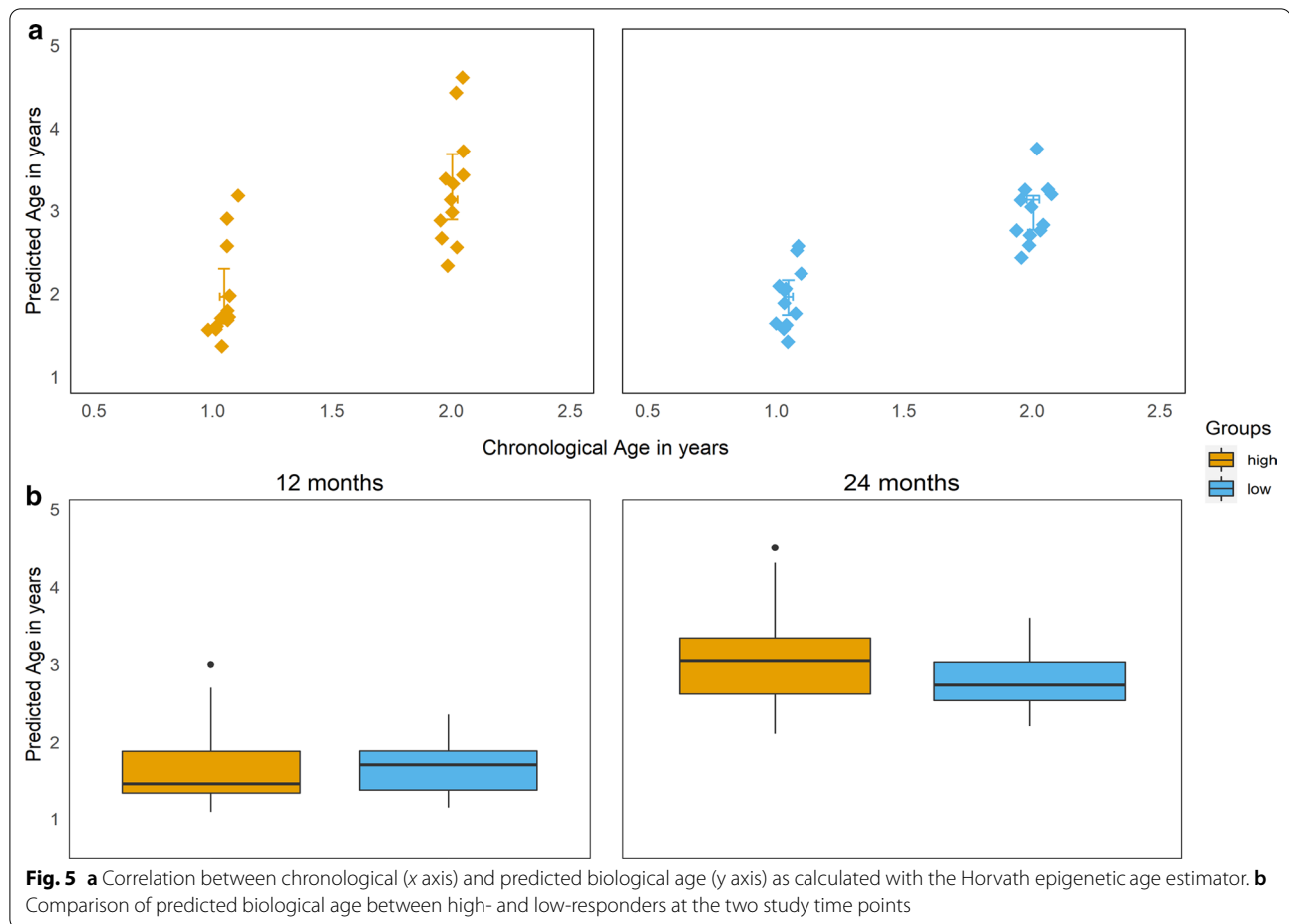
Pischedda *et al. Clin Epigenet*   (2021) 13:29

Page 8 of 12

Fig. 5 **a** Correlation between chronological (*x* axis) and predicted biological age (*y* axis) as calculated with the Horvath epigenetic age estimator. **b** Comparison of predicted biological age between high- and low-responders at the two study time points

reflect the strength of the overall immune response to immunization. Reassuringly, however, high vaccine responders showed similar patterns in OPA and memory B-cell responses, indicating that this categorization also seems to hold up in different measurements of the immune response.

Conclusion

In the present study, we have studied changes in methylation patterns of healthy children between 12 and 24 months of age and found that these involved regions dominated by immune pathways such as T cell regulation and activation. In addition, we found a number of CpGs associated with the strength of the antigen-specific IgG antibody response to a pneumococcal conjugate booster vaccine including differences in methylation patterns in *HLA-DPB1* and *IL6*. These latter findings suggest that epigenetic patterns may influence antibody responses in young children and may potentially add to their susceptibility to infection.

Methods

Study subjects and sample selection

In a previous clinical trial, 178 children were randomized to receive a booster dose of either the 10- or the 13-valent pneumococcal conjugate vaccine (PCV-13) at 12 months of age following receipt of PCV-13 at 2 and 4 months of age [19–21]. Ethical approval for this clinical vaccine trial was obtained from the Oxfordshire Research Ethics Committee (Reference number 11/SC/0473). Ethical permission to store and study genetic material was obtained prior to enrolment into the study, in accordance with the Oxford Vaccine Centre Biobank (10/H0504/25). Detailed immune responses were measured before and at 1 and 12 months after the booster. At the three study time points, anti-polysaccharide serum Immunoglobulin G (IgG) and opsonophagocytic assay (OPA) titers to all PCV-13 serotypes were determined, and antigen-specific memory B cell responses were measured for selected pneumococcal polysaccharides. For the purpose of this study, 24 individuals who had received a PCV-13 booster dose at 12 months of age ($n = 90$) (baseline group) were

Pischedda *et al. Clin Epigenet*   (2021) 13:29

Page 9 of 12

Fig. 6 **a** Principal components analysis and **b** unsupervised clustering with heatmap of 4067 differentially methylated CpG sites (uncorrected *P* value < 0.01) at 12 months of age and grouping by high and low vaccine responders. **c** Boxplots showing 4 DMPs associated with hypomethylation of *HLA-DPB1* and 2 DMPs associated with hypermethylation of *IL6* in high vaccine responders. The *y*-axis represents the *β* value for each position in both groups (yellow for high responders, light blue for low responders)

selected based on their aggregated IgG antibody response and categorized into high and low responders. For this categorization, the strength of the polysaccharide-specific IgG response was ranked for each PCV-13 recipient and vaccine serotype at 1 month following the booster. The overall IgG antibody response was then calculated by determining the median rank for all serotypes. After excluding participants with missing serum or DNA samples, 38 individuals remained, of whom the 12 high and 12 low responders were selected (Fig. 1). This categorization was also valid for post-booster serotype-specific OPA and memory B cells responses. We used Infinium Methylation 450 K to profile (1) the epigenetic differences

between two timepoints: 12 months (baseline group) and 24 months and (2) to elucidate the methylation differences between high and low PCV-13 booster vaccine responders, in order to identify pathways that show significant changes over time and those that are associated with a more robust immune response.

Laboratory procedures

Polysaccharide-specific antibody measurements were performed as previously described [19, 44]. DNA was extracted from blood clots collected from the same participants at 12 and 24 months of age. Whole blood DNA was bisulfite converted using the EZ-96 DNA Bisulfite

Pischedda *et al. Clin Epigenet*   (2021) 13:29

Page 10 of 12

Zymo Research conversion protocol according to the manufacturer's instructions. The treated DNA was then hybridized to the Illumina Infinium Methylation450K BeadChip, and the array was imaged using the Illumina iScan system in which the percent methylation state of each CpG site was quantified for the entire study group.

Data analysis

The epigenetic profile from study participants was measured at both time points using the Illumina Methylation 450 K assay covering >485,000 methylation sites per sample at single-nucleotide resolution. DNA methylation analyses were conducted using R software (v.3.6.1) and several Bioconductor packages. Raw intensity files were preprocessed and transformed into β and M values using the R package minfi. The intensities of β values were estimated from the intensity ratio of the methylated signals over the total (methylated and unmethylated) signals for each site that represents the percentage of methylation at a given cytosine for an individual across the blood cells. The β value ranges between 0 (position not methylated in any of the cells) and 1 (position methylated in all cells in the sample). The M value instead is defined as the log2 ratio of the intensities of methylated vs. unmethylated probes and indicates hypermethylation (if positive) and hypomethylation (if negative). M values close to 0 represent a similar intensity between methylated and unmethylated probes.

All raw data passed quality control and normalized using the function preprocessQuantile of the minfi package. Subsequently, to avoid artifactual data, probes with a detection P value > 0.01, probes located in sex chromosomes, probes in sites containing SNPs or with a minor allele frequency < 5% and probes known to have cross-reaction were removed. This filtering removed 28,999 leaving 456,513 probes for subsequent analysis. As the DNA samples were obtained from peripheral blood and because of the extreme cell-type specificity of DNA methylation [45], cell composition heterogeneity was evaluated [46] using the package FlowSorted.Blood.450 K and the estimateCellCounts function. Batch effect was removed using Combat from SVA package.

Identification of differentially methylated probes/positions (DMPs) between the study timepoint and high- and low-responders to the vaccine was performed using limma package [47] fitting a linear regression model to each CpGs site. M-values are more homoscedastic than β-values and were thus used for all statistical analyses because of their better detection sensitivity [48]. However, we report β-values in text and figures to facilitate interpretation. Through limma package, it was possible to include covariates in the specification of the model (M values ~ Group + Individuals + Responder + Sex + Cell Composition). Output of the linear model was further analyzed using an empirical Bayes method to moderate standard errors. P values were corrected for multiple testing using the Benjamini–Hochberg false discovery rate (FDR) method [49], and DMPs were defined as all positions with an FDR P value < 0.01. CpGs were annotated using Bioconductor package lluminaHumanMethylation450kanno.ilmn12.hg19 (v1.2) to genomic regions classified in regions 200 bp upstream of the transcription start site (TSS; TSS200), 1500 bp upstream of the TSS (TSS1500), the 5′ and 3′ untranslated regions (UTRs), 1st exon and gene body. Regions are further subdivided according to their relation to CpG-rich DNA sequences, the so-called CpG islands (CGI), in CpG N or S shelves (within ~4 kb north or south from CGI), CpG N or S shores (within ~2 kb north or south from CGI) and open sea (region >4 kb from CGI). Differentially methylated regions (DMRs) refer to genomic regions with multiple differentially methylated positions close together and with different methylation patterns across samples.

Principal component analysis (PCA) was performed to visualize global epigenome patterns comparing 12- and 24-month samples as well as samples from high and low responders. Pathway analysis was performed employing the methylglm function of the methylGSA package [50]. This function adjusts for the number of CpGs by implementing a logistic regression model using a functional class scoring method; all CpGs ranked by differential methylation test P values were considered in gene set testing since each CpGs could be of interest. Pathways enrichment was considered significant if false discovery rate (FDR) < 0.05.

Supplementary Information

The online version contains supplementary material available at https://doi.org/10.1186/s13148-021-01012-w.

Additional file 1: Figure 1. Boxplots of IgG antibody concentrations against PCV-13 serotypes (serotype indicated above each box) in low and high responders (n = 12 each; based on aggregated IgG antibody concentration 1 month post-vaccination) as well as middle responders (n = 14) and children without available DNA (n = 36).

Additional file 2: Figure 2. Boxplots of OPA antibody titers against PCV-13 serotypes (serotype indicated above each box) in low and high responders (n = 12 each; based on aggregated IgG antibody concentration 1 month post-vaccination) as well as middle responders (n = 14) and children without available DNA (n = 36).

Additional file 3: Figure 3. Boxplots of IgG antibody-secreting cell frequencies against selected PCV-13 serotypes (serotype indicated above each box) in low and high responders (n = 12 each; based on aggregated IgG antibody concentration 1 month post-vaccination) as well as middle responders (n = 14) and children without available DNA (n = 36).

Additional file 4. QQ plot of the observed *p*-values against the expected *p*-values.

Pischedda *et al. Clin Epigenet* (2021) 13:29

Page 11 of 12

Author details
[1] Genetics, Vaccines and Infections and Pediatrics Research Group (GENVIP), Instituto de Investigación Sanitaria de Santiago, Santiago de Compostela, Spain. [2] Translational Pediatrics and Infectious Diseases, Department of Pediatrics, Hospital Clínico Universitario de Santiago de Compostela, Santiago de Compostela, Spain. [3] Hospital Clínico Universitario de Santiago (SERGAS), Unidade de Xenética, Instituto de Ciencias Forenses, Facultade de Medicina, Universidade de Santiago de Compostela, and GenPoB Research Group, Instituto de Investigaciones Sanitarias (IDIS), Galicia, Spain. [4] Oxford Vaccine Group, Department of Paediatrics, University of Oxford, and The NIHR Oxford Biomedical Research Centre, Oxford, UK. [5] MRC-Weatherall Institute of Molecular Medicine, University of Oxford, Oxford, UK. [6] Division of Immunology and Children's Research Center, University Children's Hospital Zurich, University of Zurich (UZH), Zurich, Switzerland.

References
1. Blanchard-Rohner G, Pollard AJ. Long-term protection after immunization with protein–polysaccharide conjugate vaccines in infancy. Expert Rev Vaccines. 2011;10(5):673–84.
2. O'Brien KL, Wolfson LJ, Watt JP, Henkle E, Deloria-Knoll M, McCall N, et al. Burden of disease caused by *Streptococcus pneumoniae* in children younger than 5 years: global estimates. The Lancet. 2009;374(9693):893–902.
3. World Health Organization. Pneumococcal conjugate vaccine for childhood immunization—WHO position paper. Wkly Epidemiol Rec. 2007;82(12):93–104.
4. Kollmann TR, Kampmann B, Mazmanian SK, Marchant A, Levy O. Protecting the newborn and young infant from infectious diseases: lessons from immune ontogeny. Immunity. 2017;46(3):350–63.
5. Westerink MJ, Schroeder HW Jr, Nahm MH. Immune responses to pneumococcal vaccines in children and adults: rationale for age-specific vaccination. Aging Dis. 2012;3(1):51.
6. Lipsitch M, Li LM, Patterson S, Trammel J, Juergens C, Gruber WC, et al. Serotype-specific immune responses to pneumococcal conjugate vaccine among children are significantly correlated by individual: analysis of randomized controlled trial data. Vaccine. 2018;36(4):473–8.
7. Mentzer AJ, O'Connor D, Pollard AJ, Hill AV. Searching for the human genetic factors standing in the way of universally effective vaccines. Philos Trans R Soc Lond B Biol Sci. 2015;370(1671):20140341.
8. O'Connor D, Png E, Khor CC, Snape MD, Hill AVS, van der Klis F, et al. Common genetic variations associated with the persistence of immunity following childhood immunization. Cell Rep. 2019;27(11):3241–53.
9. Jones PA, Takai D. The role of DNA methylation in mammalian epigenetics. Science. 2001;293(5532):1068–70.
10. Bibikova M, Lin Z, Zhou L, Chudin E, Garcia EW, Wu B, et al. High-throughput DNA methylation profiling using universal bead arrays. Genome Res. 2006;16(3):383–93.
11. Perera F, Herbstman J. Prenatal environmental exposures, epigenetics, and disease. Reprod Toxicol. 2011;31(3):363–73.
12. Boks MP, Derks EM, Weisenberger DJ, Strengman E, Janson E, Sommer IE, et al. The relationship of DNA methylation with age, gender and genotype in twins and healthy controls. PLoS ONE. 2009;4(8):e6767.
13. Bell CG, Lowe R, Adams PD, Baccarelli AA, Beck S, Bell JT, et al. DNA methylation aging clocks: challenges and recommendations. Genome Biol. 2019;20(1):249.
14. Boulias K, Lieberman J, Greer EL. An epigenetic clock measures accelerated aging in treated HIV infection. Mol Cell. 2016;62(2):153–5.
15. Horvath S, Garagnani P, Bacalini MG, Pirazzini C, Salvioli S, Gentilini D, et al. Accelerated epigenetic aging in down syndrome. Aging Cell. 2015;14(3):491–5.
16. Fernandez-Morera JL, Calvanese V, Rodriguez-Rodero S, Menendez-Torre E, Fraga MF. Epigenetic regulation of the immune system in health and disease. Tissue Antigens. 2010;76(6):431–9.
17. Kondilis-Mangum HD, Wade PA. Epigenetics and the adaptive immune response. Mol Asp Med. 2013;34(4):813–25.
18. Acevedo N, Reinius LE, Vitezic M, Fortino V, Soderhall C, Honkanen H, et al. Age-associated DNA methylation changes in immune genes, histone modifiers and chromatin remodeling factors within 5 years after birth in human blood leukocytes. Clin Epigenet. 2015;7:34.
19. Truck J, Jawad S, Goldblatt D, Roalfe L, Snape MD, Voysey M, et al. The antibody response following a booster with either a 10- or 13-valent pneumococcal conjugate vaccine in toddlers primed with a 13-valent pneumococcal conjugate vaccine in early infancy. Pediatr Infect Dis J. 2016;35(7):787–93.
20. Truck J, Kelly S, Jawad S, Snape MD, Voysey M, Pollard AJ. Differences in immunization site pain in toddlers vaccinated with either the 10- or the 13-valent pneumococcal conjugate vaccine. Pediatr Infect Dis J. 2018;37(4):e103–6.

Pischedda *et al. Clin Epigenet*   (2021) 13:29

Page 12 of 12

21. Truck J, Snape MD, Tatangeli F, Voysey M, Yu LM, Faust SN, et al. Pneumococcal serotype-specific antibodies persist through early childhood after infant immunization: follow-up from a randomized controlled trial. PLoS ONE. 2014;9(3):e91413.

22. Horvath S. DNA methylation age of human tissues and cell types. Genome Biol. 2013;14(10):3156.

23. Arechederra M, Daian F, Yim A, Bazai SK, Richelme S, Dono R, et al. Hypermethylation of gene body CpG islands predicts high dosage of functional oncogenes in liver cancer. Nat Commun. 2018;9(1):3164.

24. Ladd-Acosta C, Hansen KD, Briem E, Fallin MD, Kaufmann WE, Feinberg AP. Common DNA methylation alterations in multiple brain regions in autism. Mol Psych. 2014;19(8):862–71.

25. Maschietto M, Rodrigues TC, Kashiwabara AY, de Araujo ÉSS, Aguiar TFM, da Costa CML, et al. DNA methylation landscape of hepatoblastomas reveals arrest at early stages of liver differentiation and cancer-related alterations. Oncotarget. 2017;8(58):97871.

26. Henry CJ, Ornelles DA, Mitchell LM, Brzoza-Lewis KL, Hiltbold EM. IL-12 produced by dendritic cells augments CD8+ T cell activation through the production of the chemokines CCL1 and CCL17. J Immunol. 2008;181(12):8576–84.

27. Martinez GJ, Zhang Z, Chung Y, Reynolds JM, Lin X, Jetten AM, et al. Smad3 differentially regulates the induction of regulatory and inflammatory T cell differentiation. J Biol Chem. 2009;284(51):35283–6.

28. Scharschmidt E, Wegener E, Heissmeyer V, Rao A, Krappmann D. Degradation of Bcl10 induced by T-cell activation negatively regulates NF-κB signaling. Mol Cell Biol. 2004;24(9):3860–73.

29. DeVries A, Wlasiuk G, Miller SJ, Bosco A, Stern DA, Lohman IC, et al. Epigenome-wide analysis links SMAD3 methylation at birth to asthma in children of asthmatic mothers. J Allergy Clin Immunol. 2017;140(2):534–42.

30. Kawai T, Akira S. Regulation of innate immune signalling pathways by the tripartite motif (TRIM) family proteins. EMBO Mol Med. 2011;3(9):513–27.

31. Lunardi A, Gaboli M, Giorgio M, Rivi R, Bygrave A, Antoniou M, et al. A role for PML in innate immunity. Genes Cancer. 2011;2(1):10–9.

32. Huang CT, Workman CJ, Flies D, Pan X, Marson AL, Zhou G, et al. Role of LAG-3 in regulatory T cells. Immunity. 2004;21(4):503–13.

33. Ovsyannikova IG, Pankratz VS, Vierkant RA, Pajewski NM, Quinn CP, Kaslow RA, et al. Human leukocyte antigens and cellular immune responses to anthrax vaccine adsorbed. Infect Immun. 2013;81(7):2584–91.

34. Lambert ND, Haralambieva IH, Kennedy RB, Ovsyannikova IG, Pankratz VS, Poland GA. Polymorphisms in HLA-DPB1 are associated with differences in rubella virus-specific humoral immunity after vaccination. J Infect Dis. 2015;211(6):898–905.

35. Yao Y, Yang H, Shi L, Liu S, Li C, Chen J, et al. HLA class II genes HLA-DRB1, HLA-DPB1, and HLA-DQB1 are associated with the antibody response to inactivated Japanese encephalitis vaccine. Front Immunol. 2019;10:428.

36. Dhiman N, Bonilla RG, Jacobson RM, O'Kane D, Poland GA. Differential HLA gene expression in measles vaccine seropositive and seronegative subjects: a pilot study. Scand J Infect Dis. 2003;35(5):332–6.

37. Sandoval J, Heyn H, Moran S, Serra-Musach J, Pujana MA, Bibikova M, et al. Validation of a DNA methylation microarray for 450,000 CpG sites in the human genome. Epigenetics. 2011;6(6):692–702.

38. Consortium EP. An integrated encyclopedia of DNA elements in the human genome. Nature. 2012;489(7414):57–74.

39. Jones SA. Directing transition from innate to acquired immunity: defining a role for IL-6. J Immunol. 2005;175(6):3463–8.

40. Su L-K, Yu F, Li Z-F, Zeng C, Xu Q-A, Fan M-W. Intranasal co-delivery of IL-6 gene enhances the immunogenicity of anti-caries DNA vaccine. Acta Pharmacol Sin. 2014;35(5):592–8.

41. Su B, Wang J, Wang X, Jin H, Zhao G, Ding Z, et al. The effects of IL-6 and TNF-α as molecular adjuvants on immune responses to FMDV and maturation of dendritic cells by DNA vaccination. Vaccine. 2008;26(40):5111–22.

42. Kurtz SL, Foreman O, Bosio CM, Anver MR, Elkins KL. Interleukin-6 is essential for primary resistance to Francisella tularensis live vaccine strain infection. Infect Immun. 2013;81(2):585–97.

43. Velazquez-Salinas L, Verdugo-Rodriguez A, Rodriguez LL, Borca MV. The role of interleukin 6 during viral infections. Front Microbiol. 2019;10:1057.

44. Truck J, Mitchell R, Jawad S, Clutterbuck EA, Snape MD, Kelly DF, et al. Divergent memory B cell responses in a mixed infant pneumococcal conjugate vaccine schedule. Pediatr Infect Dis J. 2017;36(5):e130–5.

45. Ziller MJ, Gu H, Muller F, Donaghey J, Tsai LT, Kohlbacher O, et al. Charting a dynamic DNA methylation landscape of the human genome. Nature. 2013;500(7463):477–81.

46. Houseman EA, Accomando WP, Koestler DC, Christensen BC, Marsit CJ, Nelson HH, et al. DNA methylation arrays as surrogate measures of cell mixture distribution. BMC Bioinform. 2012;13:86.

47. Smyth GK. Limma: linear models for microarray data. Bioinformatics and computational biology solutions using R and Bioconductor. New York: Springer; 2005. p. 397–420.

48. Du P, Zhang X, Huang CC, Jafari N, Kibbe WA, Hou L, et al. Comparison of Beta-value and M-value methods for quantifying methylation levels by microarray analysis. BMC Bioinform. 2010;11:587.

49. Benjamini Y, Hochberg Y. Controlling the false discovery rate: a practical and powerful approach to multiple testing. J R Stat Soc Ser B (Methodol). 1995;57(1):289–300.

50. Ren X, Kuan PF. methylGSA: a Bioconductor package and Shiny app for DNA methylation data length bias adjustment in gene set testing. Bioinformatics. 2019;35(11):1958–9.

Publisher's Note